Edge effects on tree architecture exacerbate biomass loss of fragmented Amazonian forests

Matheus Nunes (matheus.nunes@helsinki.fi)
University of Helsinki https://orcid.org/0000-0001-9979-6456

Marcel Vaz
Wilkes University

José Luís Camargo
Biological Dynamics of Forest Fragment Project (INPA & STRI) https://orcid.org/0000-0003-0370-9878

William Laurance
James Cook University https://orcid.org/0000-0003-4430-9408

Ana de Andrade
Instituto Nacional de Pesquisas da Amazônia https://orcid.org/0000-0001-8550-1127

Alberto Vicentini
National Institute for Amazonian Research

Susan Laurance
James Cook University https://orcid.org/0000-0002-2831-2933

Pasi Raumonen
Tampere University https://orcid.org/0000-0001-5471-0970

Toby Jackson
University of Oxford https://orcid.org/0000-0001-8143-6161

Gabriela Zuquim
University of Turku

JIn Wu
University of Hong Kong https://orcid.org/0000-0001-8991-3970

Josep Penuelas
CSIC, Global Ecology Unit CREAF-CSIC-UAB, Cerdanyola del Vallès 08193, Catalonia, Spain
https://orcid.org/0000-0002-7215-0150

Jerome Chave
CNRS, Université Paul Sabatier https://orcid.org/0000-0002-7766-1347

Eduardo Maeda
University of Helsinki https://orcid.org/0000-0001-7932-1824

Article

Keywords:

Posted Date: May 5th, 2023

DOI: https://doi.org/10.21203/rs.3.rs-2855410/v1

Additional Declarations: There is **NO** Competing Interest.

Edge effects on tree architecture exacerbate biomass loss of fragmented Amazonian forests

Matheus Henrique Nunes [1, 15], Marcel Caritá Vaz [2], José Luís Campana Camargo [3, 4], William F. Laurance [5], Ana Andrade, [4] Alberto Vicentini [4, 6], Susan Laurance [5], Pasi Raumonen [7], Tobias Jackson [8], Gabriela Zuquim [9], Jin Wu [10], Josep Peñuelas [11, 12], Jérôme Chave [13], Eduardo Eiji Maeda [1, 14, 15]

AFFILIATIONS

[1] Department of Geosciences and Geography, P.O. Box 68, FI-00014 University of Helsinki, Helsinki, Finland

[2] Institute for Environmental Science and Sustainabilty, Wilkes University, 84 W. South St. Box 91, Wilkes-Barre, PA 18766, U.S.A.

[3] Ecology Graduate Program, National Institute for Amazonian Research, (INPA), Manaus, Brazil

[4] Biological Dynamics of Forest Fragments Project (BDFFP) at National Institute for Amazonian Research (INPA), Manaus, Brazil.

[5] Centre for Tropical Environmental and Sustainability Science, College of Science and Engineering, James Cook University, Cairns, Queensland 4878, Australia

[6] Coordenação de Pesquisas em Ecologia, Instituto Nacional de Pesquisas da Amazônia (INPA), Manaus, AM, Brasil

[7] Computing Sciences, Tampere University, Korkeakoulunkatu 3, 33720, Tampere, Finland

[8] Plant Sciences and Conservation Research Institute, University of Cambridge, Cambridge, CB2 3QZ, United Kingdom

[9] Amazon Research Team, Department of Biology, University of Turku, Finland

[10] School of Biological Sciences and Institute for Climate and Carbon Neutrality, The University of Hong Kong, Pokfulam Road, Hong Kong, China

[11] CREAF, Cerdanyola del Vallès, Barcelona 08193, Catalonia, Spain.

[12] CSIC, Global Ecology Unit CREAF-CSIC-UAB, Bellaterra, Barcelona 08193, Catalonia, Spain.

[13] Laboratoire Evolution et Diversité Biologique, CNRS, UPS, IRD, Université Paul Sabatier, Toulouse, France

[14] Finnish Meteorological Institute, FMI, Helsinki, Finland

[15] Corresponding authors

ABSTRACT

Trees adjust their architecture to acclimate to various external stressors, which regulates ecological functions that are needed for growth, reproduction, and survival. Human activities, however, are fragmenting natural habitats apace and could affect tree architecture and allometry, but quantitative assessments remain lacking. Here, we leverage ground surveys of terrestrial LiDAR in Central Amazonia to comprehensively assess forest edge effects on tree architecture and allometry, and their associated impacts on the forest biomass 40 years after fragmentation. We found that young trees colonising the forest fragments have thicker branches and architectural traits that maximise light capture, and can produce 50% more wood than their counterparts of similar stem size and height in interior forests. Large trees that have survived disturbances arising from forest fragmentation are able to acclimate and maintain their wood production, but damages that reduce tree height near the edges can lead to a 30% decline of their woody volume. Despite the large wood production of colonising trees, changes in tree architecture lead to a net loss of 6.6 Mg ha^{-1} of the forest aboveground biomass, which account for 20% of all edge-related aboveground biomass losses of fragmented Amazonian forests (34.3 Mg ha^{-1}). Our findings show a strong influence of edge effects on tree architecture and allometry, and reveal an additional unaccounted factor that exacerbates carbon losses in fragmented forests.

INTRODUCTION

The three-dimensional form of trees, defined here as tree architecture, reflects the allocation of photosynthetically fixed carbon within the plants. Tree architecture may be considered a by-product of environmental pressures on plant performance, namely growth, reproduction and survival [1,2]. Fine adjustments of the aboveground architecture of trees can minimise competition from neighbouring trees, improve hydraulic conductance, limit transpiration and maximise light capture [3–8]. In Amazonian forests, trees vary greatly in size and architecture across species, as a result of evolutionary processes over millions of years [9–11]. Size and architecture also vary considerably across individuals due to short- to mid-term acclimation and adaptation to changing environmental conditions, including canopy gaps caused by the mortality of large trees and forest blowdowns [6,12–15]. The architectural traits of Amazonian trees control CO_2 loss from stem and branch respiration, hydraulic safety and efficiency, light capture and mechanical stability, which together modulate biomass allocation and carbon storage [16–19]. Changes in tree architecture therefore could be the fingerprint of biome-wide impacts on carbon cycling, with regional and global influences on vegetation feedbacks [1,9,20,21].

The architecture of Amazonian trees could be affected by disturbances arising from forest fragmentation. The edges of forest fragments tend to have greater light availability after the mortality of large trees and lateral

light penetrating from the edges [22–24]. This may induce changes in tree architecture to optimise the capture and use of light under new circumstances, including higher vertical and horizontal crown growth that modify branching patterns and crown shape [17,25,26]. Higher temperatures and lower water availability in forest edges increase the evaporative demand of the vegetation [27,28], and trees can shorten the distances for transporting water and nutrients to minimise hydraulic conductance[7]. High wind turbulence near the fragment edges may kill highly asymmetrical trees that deviate their centre of gravity substantially from their stems [29,30]. On the other hand, highly symmetrical trees can have greater mechanical stability but a limited ability to avoid competition for light with neighbouring trees that can fit their crowns into irregular spaces. To complicate matters further, the high mortality of large individuals can damage neighbouring trees, and can result in suppressed aboveground biomass allocation of surviving trees, with large effects on the architecture and size of trees [31]. However, large uncertainties remain regarding the effects of forest fragmentation on tree architecture, particularly because i) tree architecture varies considerably across life stages [32] ii) multiple architectural attributes interact to affect the structural complexity of individual trees [2] and iii) the responses of trees to forest fragmentation vary enormously within and between species [33].

Edge effects on tree architecture could alter the woody volume of individual trees with consequences on the aboveground biomass (AGB) of fragmented Amazonian forests. There is, however, substantial uncertainties as to how tree architecture could affect allometric equations for predicting woody volume as a function of more easily measurable properties of stem diameter (DBH, diameter at breast height) and tree height, and how these allometric relationships can shape the forest AGB [34]. Forest fragments in central Amazonia experience a dramatic loss of aboveground tree biomass caused by the mortality of large trees that is not offset by the growth and recruitment of new trees [22,23]. However, little is known how differences in tree allometry caused by edge effects could either exacerbate or offset this carbon loss in fragmented forests. Allometric impacts on AGB are primarily dependent on edge effects on tree density, distribution of tree size, species composition and measurement quality of tree architecture. Terrestrial laser scanning (TLS) or "terrestrial LiDAR" surveys can be of particular importance to reduce uncertainties in tree volume estimates by considering the geometry and shape of trees, and without the difficulties associated with traditional destructive methods of tree measurement [34]. Amazonian forests are becoming more fragmented and forest edges are predicted to become a large fraction of the total forest area [35,36]. Understanding how forest edge trees adjust their architecture and allometry is therefore crucial for predicting how plants may acclimate to and survive environmental changes, and their impacts on biogeochemical fluxes and on the terrestrial carbon cycle.

Here, we tested the hypotheses that: (1) both pre-existing trees established before forest fragmentation and trees that colonised the forest fragments had their architectural traits and allometry affected by forest edges, given the higher light availability [24], higher wind turbulence [29], the hotter and drier conditions near these forest edges [28] and the high mortality of large trees that may damage their neighbours [23]; and (2) the AGB of fragmented forests is impacted by edge effects on tree allometry, with potentially significant biome-wide implications. To address these questions, we investigate the long-term edge effects on tree architecture and

tree allometry 40 years after forest fragmentation, and how changes in tree allometry impact the AGB of fragmented Amazonian forests. To quantify the edge effects on tree architecture, we conducted fieldwork in the Biological Dynamics of Forest Fragments Project (BDFFP) in Central Amazonia, the world's longest-running experimental study of habitat fragmentation [37]. We used terrestrial laser scanning (TLS, or "terrestrial LiDAR") surveys to offer new perspectives into the three-dimensional (3D) structure of trees (Figure 1), including fine-scale architectural traits [2,38] and accurate tree allometry estimates [39]. We then used more than 10,000 DBH measurements to quantify the impacts of fragmentation-related allometric changes on the forest AGB. To our knowledge, this is the first study to analyse the effects of forest fragmentation on the architecture and allometry of trees with high-resolution 3D measurements, and the first to show how the impacts of forest edges on tree architecture affect forest biomass estimates across larger spatial scales.

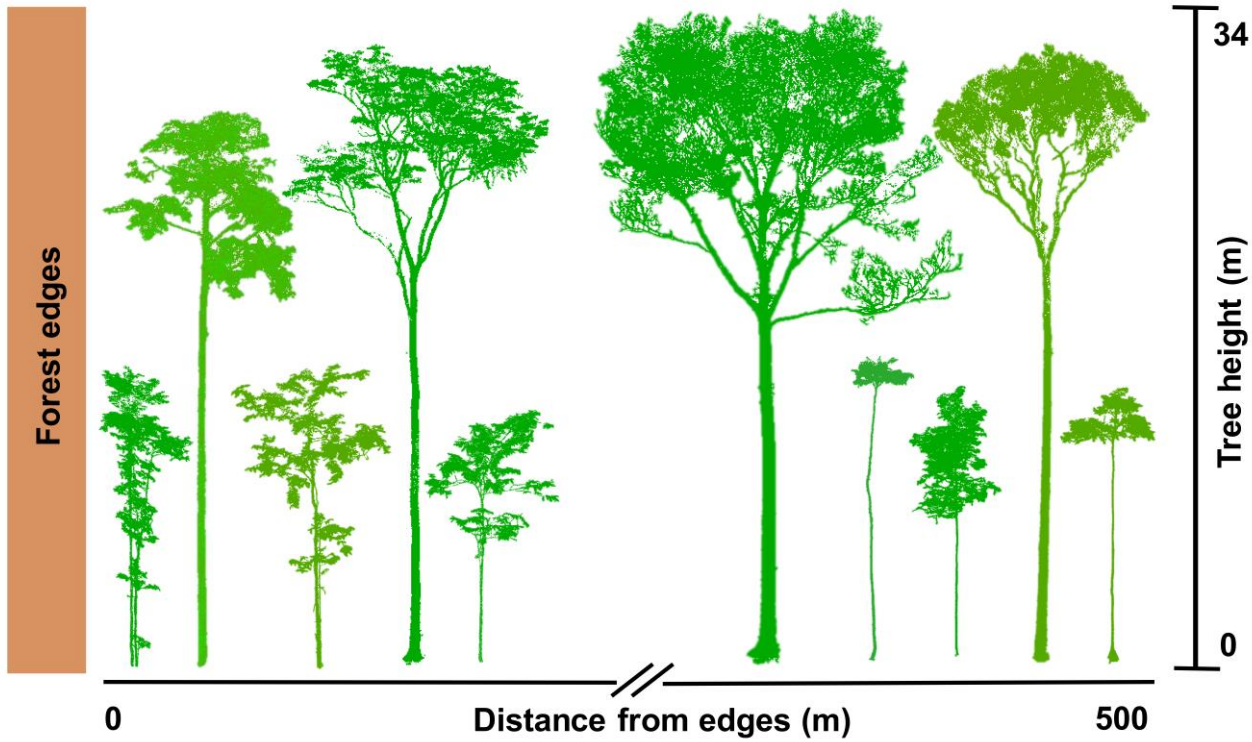

Figure 1. Point cloud of trees growing in fragmented forests in Central Amazonia, obtained using high-resolution terrestrial laser scanning (TLS). The quantification of architectural attributes of tropical trees is challenging and has been largely overlooked (Malhi et al. 2018). TLS offers new perspectives into the three-dimensional (3D) structure of trees, including descriptions of fine-scale architectural traits such as tree asymmetry and vertical distribution of branches. Here, we investigate how the architecture of surviving and young colonising trees change with proximity to forest edges. We used TLS data that resulted in a point spacing of 1.4 cm at a 20 m distance from the scanner.

RESULTS

Edge effects on architectural traits

We used tree height to determine whether trees have been established before or after forest fragmentation. Trees above 20 m in height were considered to have established before the forest fragmentation in 1980 and thus have survived the 40-year-old edge effects. Trees below 20 m in height were most likely post-fragmentation recruits (Supplementary Figure 4). Edge effects on architectural traits varied widely in extent, with trait changes most pronounced between 10 and 55 m from the forest margins (Supplementary Figure 5). We then used edges versus interior based on this extent for each architectural trait.

Our models demonstrated that edge effects interacted with tree height to influence architectural traits (Figure 2). The surviving tall trees in the edges had higher surface area per unit volume of trunks ($CI_{95\%}$: 24 - 26 m^2 m^{-3} in the edge *vs.* $CI_{95\%}$: 14 - 16 m^2 m^{-3} in the interior), which demonstrates that edge effects led to thinner trunks (as thinner objects have a higher area area per unit volume). Tall trees were more symmetrical in the edges than in the interior forests ($CI_{95\%}$: 14 - 18 in the edge *vs.* 11 - 13 in the interior) and had a reduced path fraction ($CI_{95\%}$: 0.63 - 0.67 in the edge *vs.* 0.69 - 0.73 in the interior). Relative crown width ($CI_{95\%}$: 0.20 - 0.29 m cm^{-1} in the edges *vs.* 0.25 - 0.27 m cm^{-1} in the interior) and relative crown depth ($CI_{95\%}$: 0.45 - 0.65 m m^{-1} in the edges *vs.* 0.51 - 0.56 m m^{-1}in the interior) in the edges were not distinct from those of interior forests, indicating that crown dimensions in the edges were proportional to trunk size and tree height compared to trees in the interior.

Our results also demonstrate that short trees in the forest edges had thicker branches and trunks, owing to reduced branch surface area per unit volume ($CI_{95\%}$: 170 - 200 m^2 m^{-3} in the edges *vs.* 250 - 400 m^2 m^{-3} in the interior) and trunk surface area per unit volume ($CI_{95\%}$: 74 - 77 m^2 m^{-3} in the edges *vs.* 80 - 100 m^2 m^{-3} in the interior), trees were more asymmetrical ($CI_{95\%}$: 3.0 - 3.2 in the edges *vs.* 2.0 - 2.5 in the interior) and had higher path fraction ($CI_{95\%}$: 0.59 - 0.63 in the edges *vs.* 0.53 - 0.57 in the interior). The crown of small trees in the edges had larger relative depth most possibly owing to multi-stemmed trees that colonised the forest edges ($CI_{95\%}$: 0.60 - 0.75 m m^{-1} in the edges *vs.* 0.50 - 0.55 m m^{-1} in the interior), but smaller relative width given the large trunk sizes of short trees in the forest edges ($CI_{95\%}$: 0.41 - 0.50 m cm^{-1} in the edges *vs.* 0.51 - 0.56 m cm^{-1} in the interior).

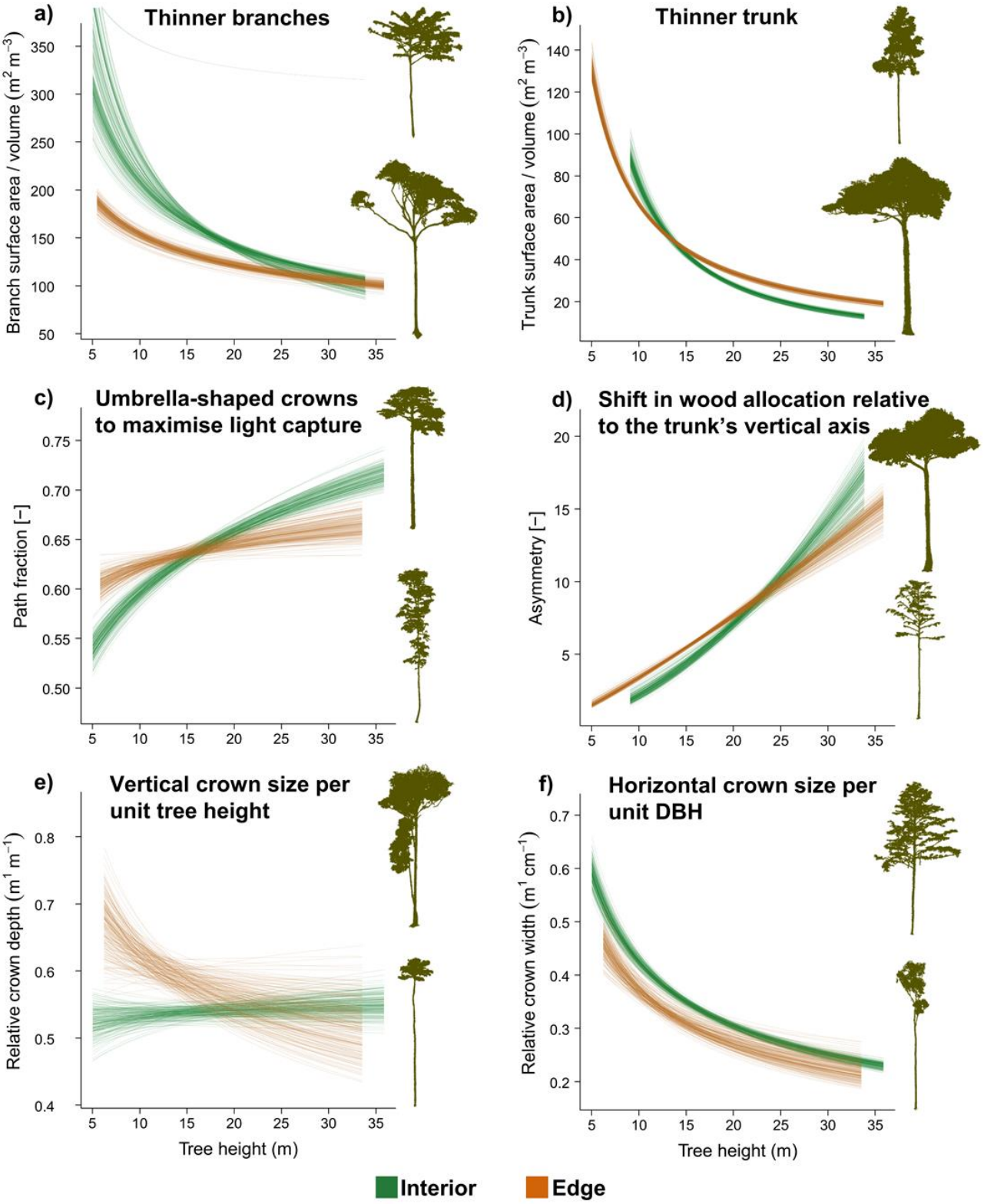

Figure 2. Tree architectural traits acquired using a Terrestrial Laser Scanner (TLS) within the Biological Dynamics of Forest Fragments Project (BDFFP) in Central Amazonia varied with tree height and were affected by edge effects. Predictions from nonlinear mixed modelling used tree height, a categorical variable that indicates whether plots were near an edge (edge effects) and an interaction term (tree height × edge effects) as fixed variables. Plot identity nested within landscape (position of fragment within the landscape and fragment size) and region within Central Amazonia were included as random variables. a) Predicted

surface area per unit volume (m^2 m^{-3}) of branches, b) predicted surface area per unit volume (m^2 m^{-3}) of trunks, c) predicted path fraction, d) predicted asymmetry, e) predicted relative crown depth (m m^{-1}, measured as crown height divided by tree height), and f) predicted relative crown width (m cm^{-1}, measured as crown width divided by the trunk diameter at breast height - DBH) of trees in forest edges (orange) and forest interior (green). Each line corresponds to the model prediction obtained by fitting 200 randomised permutations of subsets split into 80/20 for calibration and validation, respectively. Plot titles indicate the ecological meaning of high trait values. TLS-based trees are shown for a visual representation of the variation between low and high trait values.

Architectural traits, except relative crown depth, were correlated with the woody volume of individual trees (Supplementary Figure 7) and one component of variation tightly linked to variation in woody volume explained nearly half of all the changes in architectural traits (Supplementary methods 5; Supplementary Figure 8). Trees with thicker branches and trunks, as well as those who had a small relative crown width, given their large trunk sizes, had higher woody volume. These high-volume trees tended to be more asymmetrical and higher path fraction.

Edge effects on tree allometry

We developed allometric equations for trees in the forest interior and forest edges that predict the aboveground woody volume as a function of stem size and tree height (DBH^2 x H) (Eq. 1 and 2) or as a function of DBH only (Eq. 3 and 4) for trees in the forest interior and forest edges. Effects of fine-scale architectural variation on allometric relationships (Eq. 1 and 2) were pronounced within the first 76 from the forest edges, whereas edge effects on Eq. 3 and 4 with woody volume as a function of DBH only were most pronounced within the first 55 m from the forest fragment margins (Supplementary Figure 9a, 9b). While equations 1 and 2 reflect differences in allocation patterns at the trunk and branch levels caused by fine-scale architectural variation, including thinning or thickening of branches and trunks, branch loss and changes in branch length, equations 3 and 4 also capture edge effects on tree height, including height growth or height reduction from damages to living trees (i.e., stem breakage).

We observed that for a given DBH and height, the surviving tall trees in the edges had similar aboveground woody volume as their counterparts in the forest interior, while the short colonising trees had larger woody volume than recruits in the forest interior (Figure 3a). These allometric relationships were also valid for the compartmentalised volume in trunks and branches (Supplementary Figures 10a, 10b). Predictions of the woody volume as a function of DBH only revealed an additional factor modulating the woody volume of individual trees caused by variation in tree height. Relationships between DBH and tree height demonstrate that a considerable fraction of trees near the edges had a large reduction in height for a given stem size (Supplementary Figure 11). Thereby, the reduced aboveground woody volume of the surviving trees in the

edges when predicted as a function of DBH is probably caused by the decrease in height on some trees (Figure 3b), considering the non-significant edge effects on the woody volume caused by fine-scale architectural variation.

We then illustrate these fragmentation effects on allometric relationships for predicting woody volume as a function of DBH^2 x H. For example, a surviving tree with 33 m height and 70 cm DBH is predicted to have a woody volume of 7.7 m^3 in interior forests and 7.4 m^3 in the forest edges, a non-significant variation in the woody volume of surviving trees related to edge effects on fine-scale architectural traits ($CI_{95\%}$: 7.3 - 8.0 in the interior *vs.* 7.0 - 8.0 in the edges). A colonising tree with 10 m height and 10 cm DBH is predicted to have a woody volume of 0.12 m^3 in the interior and 0.18 m^3 in edges, an increase of 50% in the woody volume caused by edge effects on fine-scale architectural traits. However, when woody volume is predicted as a function of DBH only, a 70 cm DBH tree in the interior is predicted to have a woody volume of 8.14 m^3, but edge effects reduce a surviving 70 cm DBH tree to a volume of 6.27 m^3, a 30% decline in its woody volume.

$$\ln(\text{Woody volume}_{\text{interior}}) = -0.21 + 0.81 \ln(DBH^2 H_{\text{interior}}) + \varepsilon_i \quad \textbf{(Eq. 1)}$$

$$\ln(\text{Woody volume}_{\text{edge}}) = -0.13 + 0.72 \ln(DBH^2 H_{\text{edge}}) + 0.016 \ln(DBH^2 H_{\text{edge}})^2 + \varepsilon_i \quad \textbf{(Eq. 2)}$$

$$\ln(\text{Woody volume}_{\text{interior}}) = 2.80 + 1.97 \ln(DBH_{\text{interior}}) + \varepsilon_i \quad \textbf{(Eq. 3)}$$

$$\ln(\text{Woody volume}_{\text{edge}}) = 2.45 + 1.72 \ln(DBH_{\text{edge}}) + \varepsilon_i \quad \textbf{(Eq. 4)}$$

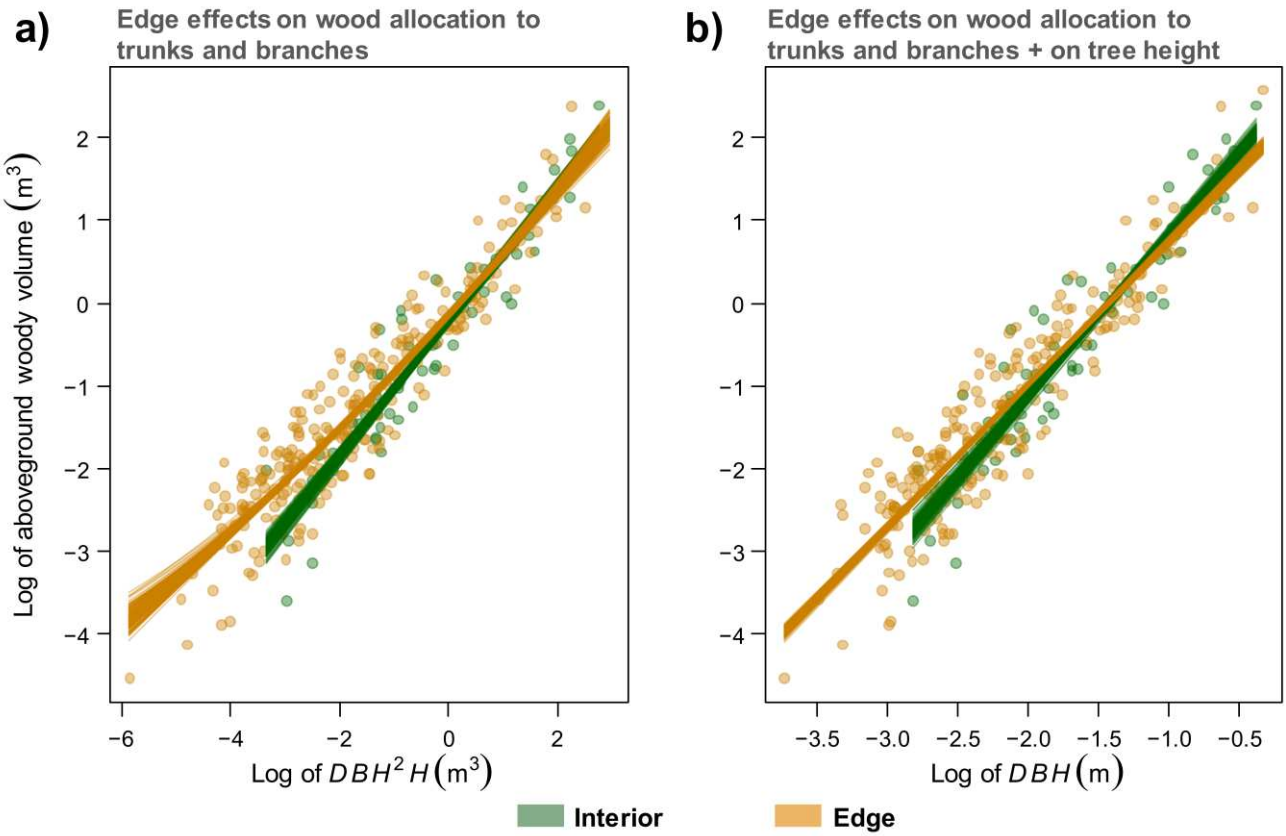

Figure 3. Linear mixed model regressions that predict the logarithm of aboveground volume (m^3) as a function of a) the logarithm of $DBH^2 H$ (m^3) and b) the logarithm of DBH (m) for trees in forest edges (orange) and forest interior (green). DBH is the diameter at breast height measured at 1.3 m above the ground in metres, and H is the total tree height in metres. Tree measurements were acquired using a Terrestrial Laser Scanner (TLS) within the Biological Dynamics of Forest Fragments Project (BDFFP) in Central Amazonia. Plot identity nested within landscape (position of fragment within the landscape and fragment size) and region within Central Amazonia were included as random variables. Points represent the observed values and each line corresponds to the model prediction obtained by fitting 200 randomised permutations of subsets split into 80/20 for calibration and validation, respectively.

Edge effects on AGB estimates across larger-spatial scales

We investigated whether the increased woody volume of understory colonising trees in the forest edges (an increase of up to 50%) may offset the loss of woody volume of the large surviving trees caused by their reduction in height (up to a 30% decline). We compared AGB estimates within 55 m from the forest margins comparing estimates from Eq.3 and Eq.4 to predict the impacts of edge effects on tree allometry and their associated effects on the forest AGB.

Our findings reveal that edge effects on tree allometry have significant impacts on the forest AGB (Figure 4). We found that within 100 m from the forest margins, AGB is reduced by 34.3 Mg ha^{-1} ($F = 775.3$, P-value < 0.00001). This value corresponds to an 11.4% reduction in AGB due to the combined edge effects on forest

structure (owing to changes in tree size, tree density and species composition) in comparison to interior forests AGB (27.7 Mg ha^{-1}) and on tree allometry (6.6 Mg ha^{-1}). These values report on a significant impact arising from edge effects on tree allometry that corresponds to one-fifth (20%) of all AGB losses from forest fragmentation.

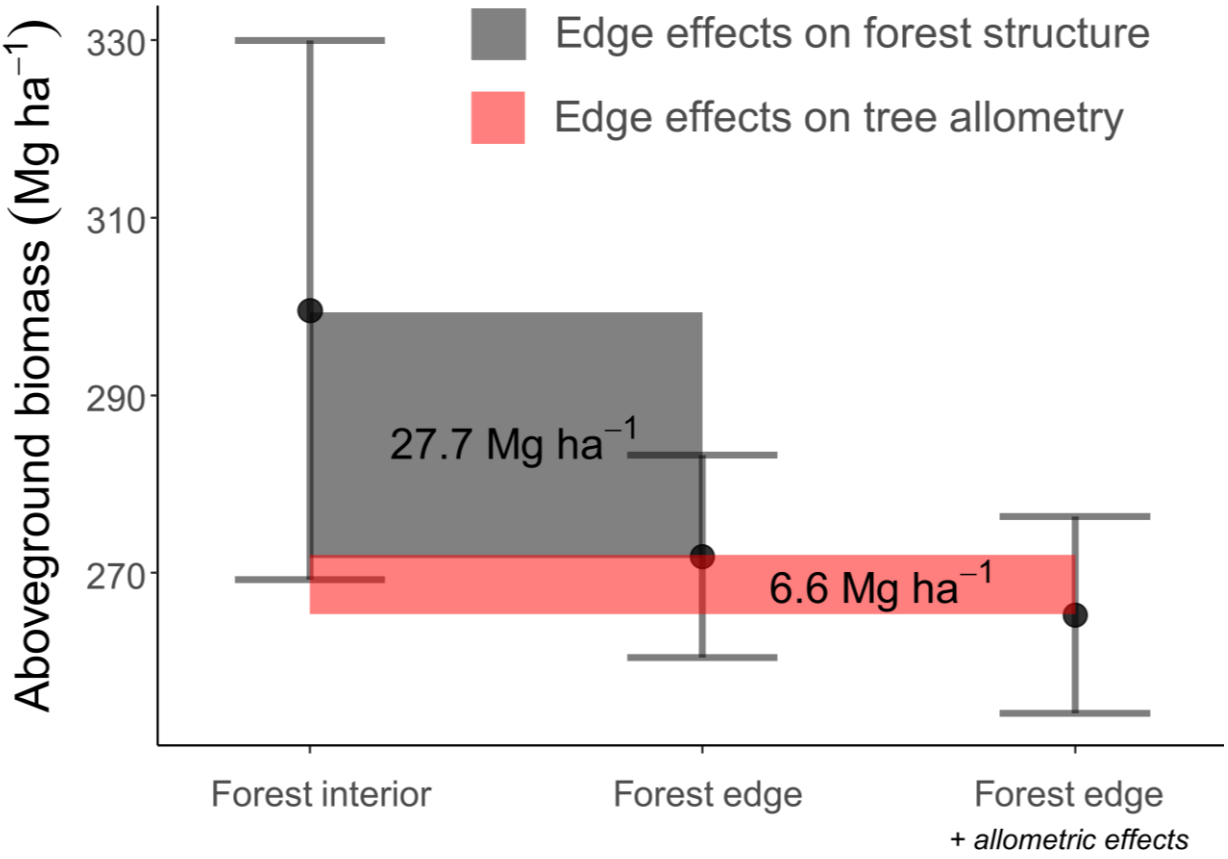

Figure 4. Plot-level median aboveground biomass (AGB) for edge (N = 30 ha) versus interior (N = 6 ha) forest plots within the Biological Dynamics of Forest Fragments Project (BDFFP) in Central Amazonia. Error bars denote 95% confidence intervals. The 36 1-ha plots contained tree measurements on more than 10,000 individual stems ≥10 cm diameter across 963 tree species. The shaded dark grey area corresponds to the edge effects on AGB caused by changes in the forest structure owing to edge effects on tree mortality, growth and recruitment. The shaded red area corresponds to the edge effects on AGB caused by changes in tree allometry with forest fragmentation.

DISCUSSION

High density terrestrial LiDAR combined with long-term tree measurements across Central Amazonia provided a fresh perspective on the architecture and allometry of trees and their associated impacts on the aboveground biomass of forest fragments. Pre-existing trees that have survived 40 years of edge effects have the ability to maintain their woody volume of trunks and branches, but a reduction in height of trees near the

edges can lead to reduced woody volume. Colonising trees established after forest fragmentation, instead, have allocated more wood to branches and have produced deeper and asymmetrical crowns that may favour light capture. We found that edge effects on tree architecture impacted allometric relationships for predicting woody volume as a function of stem size, and despite the large biomass allocation in the aboveground compartments of young trees, the loss in height of tall surviving trees near the edges led to a decline in the aboveground biomass of forest fragments. We estimated an overall 11.4% reduction in AGB (34.3 Mg ha^{-1}) owing to edge effects on the forest structure (caused by mortality, growth and recruitment of trees, 27.7 Mg ha^{-1}) and tree allometry (6.6 Mg ha^{-1}). These numbers indicate that altered tree allometry alone accounted for one-fifth (20%) of all biomass losses caused by edge effects. These findings demonstrate the value of terrestrial LiDAR surveys to challenge some of the assumptions about how much carbon trees store, and to allow the detection of fine-scale changes in tree architecture. 3D measurements of tree size and shape provide a perspective on forest structure and its spatial variability that is difficult to achieve with destructive methods of tree measurement [2,39].

Terrestrial LiDAR measurements of tree architecture demonstrate that forest fragmentation had strong edge effects on architectural traits relative to trees in structurally-intact forests. However, these effects were primarily dependent on which stage of their lives trees started experiencing edge effects. Tall trees above 20 m height were established before forest fragmentation in 1980 and therefore have survived the edge effects. These surviving trees were able to allocate a similar amount of wood to branches and trunks in comparison to trees in interior forests (Supplementary Figures 10a, 10b). The forest edges of our study can have temperatures 5°C hotter and lower water availability, which lead to higher branch loss near the edges[28]. However, the similar surface area of branches per unit volume in both edge and interior forests, combined with the unaltered woody volume in branches and trunks suggest that surviving trees have the ability to maintain their woody volume, possibly by producing new branches (resprouting) that has positive influences on tree growth and survival [40]. The tall trees in the edges also had lower path fraction and were more symmetrical than trees in interior forests. In fact, trees under stress can lose terminal branches[41], with the remaining branches shorter in path length to increase hydraulic safety by decreasing the length that water and nutrients need to travel for photosynthesis [7,42]. The observed higher symmetry of surviving trees near the edges can increase their mechanical stability to high air turbulence caused by strong winds in the forest edges [29,30,43,44]. These results suggest that surviving trees had mechanisms of acclimation to stressful conditions near the forest edges - in particular higher temperatures, lower water availability, stronger winds, with minimal effects on allocation of biomass to the aboveground compartments. However, a complementary explanation could be that edge effects selected for individuals or species that were more adapted to the edge conditions. Indeed, forest fragmentation has led to a high mortality rate of tall trees [23], and the surviving trees may be those with traits that provide better individual's fitness to the micro-environmental conditions near the forest edges. Better understanding the intra-specific controls can help us predict variation in tree architecture with forest fragmentation in the Amazon.

The new recruits that colonised the forest fragments, instead, were more adapted to maximise light capture given their higher amount of woody volume in the branches and trunks, higher asymmetry and higher path fraction. The forest edges had multi-stemmed trees with deeper crowns because of the high light availability near the edges [17]. Trees near the edges were more asymmetrical which may help them escape competition with their neighbours for light by shifting their biomass towards the forest edges [45]. However, this can come at the expense of lower mechanical stability [44], and trees must increase the volume of trunks prior to inducing asymmetry to avoid crown damage [46], a high predictor of tree mortality in fragmented Amazonian forests [19]. These colonising trees also produced numerous branches of high path lengths; high path lengths and path fraction may lead to lower hydraulic efficiency, as these umbrella-shaped trees have longer paths to transport water and nutrients for photosynthesis [7]. These architectural changes, alongside a large production of new leaves throughout the year [28], may explain the increased growth rates of understory tree species in the forest edges of the BDFFP project in comparison to the same tree species growing in the understory of interior forests [47], despite the hot temperatures and lower water availability in the forest edges [28]. These results indicate the ability of colonising trees in forest fragments to capture light and grow, which demonstrates the importance of protecting forest fragments for carbon cycling. However, will these colonising trees be able to grow tall and have high rates of survival in the future? These traits that maximise construction costs (i.e. high asymmetry and high path fraction) in the light-rich environments near the edges may lead to higher risks of mechanical damage and hydraulic failure. Additionally, as trees grow taller, increasing leaf water stress due to gravity and path length resistance can limit leaf expansion and photosynthesis, and consequently limit further height growth [48]. Long-term monitoring of tree architecture in controlled fragmentation experiments, including the BDFFP, is crucial to predict how these understory trees may survive in fragmented forests when they grow older and – at times- taller.

Architectural traits controlled allometric relationships for predicting the woody volume as a function of stem diameter and tree height. Trees with high woody volume were those with thick branches and trunks, and were the result of a structural adjustment under new environmental conditions in the forest edges that allows optimal light capture, including high asymmetry and path fraction (Supplementary Figure 8). Even though trees in the edges had a higher relative crown depth and higher woody volume, we did not find any evidence that relative crown depth shapes the woody volume of trees. These findings suggest that relative crown depth is a response to high-light environments to maximise lateral sunlight exposure without increasing construction costs [17], whereas trees with high asymmetry and high path fraction prioritise sun exposure and light capture but are structurally expensive to build [10,46]. Our findings demonstrate that surviving trees were able to maintain their wood production under edge effects that led to changes in architectural traits. However, our findings indicate that a large fraction of tall trees had their height strongly reduced (Supplementary Figure 11), with up to a 30% decline of their woody volume. Fragmentation of Central Amazonian forests induce mortality of large trees and branch loss [23,28] which can have pronounced impacts on neighbouring trees, with physical impacts from collateral damage [31,49]. These results suggest that stem breakage from damages caused by neighbouring trees is a strong factor driving biomass loss, which aligns with the significant negative effects of tree damage

on tree biomass [31]. Architectural differences in colonising trees, instead, led to woody volumes up to 50% higher than trees of the same stem diameter and height, demonstrating the potential of young trees in fragmented forests to offset the biomass loss caused by stem breakage of large trees. Our findings that edge effects can affect allometric relationships of Amazonian forests challenge studies that have used the same allometric equations in both fragmented and old-growth forests to estimate forest fragmentation impacts on carbon loss [22,35]. Allometric models developed for old-growth forests, if applied in forests under edge effects, can result in overestimation of the woody volume of large canopy trees (if the edge effects on tree height are not considered), and underestimation of the woody volume of small understory trees (because of large wood production with thicker trunks and branches).

We observed a 11.4% reduction (34.3 Mg ha^{-1}) in the forest AGB within the first 100 m in the forest fragments owing to changes i) in forest structure within the first 100 m from the forest edges – the combined effects of tree mortality, growth and recruitment - and ii) in tree allometry within 55 m from the forest edges. Previous studies have shown that forest fragmentation increases the mortality of large trees [22,50,51], but can also lead to higher growth rates of large trees and the recruitment of new individuals [52]. The mortality of large trees, however, represents a large fraction of the biomass loss and contributes to the high carbon emissions of fragmented ecosystems [22,35,53] Forest fragments under edge effects tend to have temperatures 3–5 °C higher and reduced soil moisture [28] which create periods of higher evaporative demand and intensify the risk of hydraulic failure of large trees[54]. Our findings also indicate that edge effects on micro-environmental conditions affect tree size, architecture and allometry. AGB losses caused by variations in tree allometry alone accounted for 6.6 Mg ha^{-1}, which is one-fifth (20%) of all AGB losses near the forest edges - a value that has been unquantified. The AGB decline caused by potential tree damage to some tall surviving trees have not been offset by the enhanced biomass of new trees colonising the forest fragments, and thereby have exacerbated the negative edge effects on AGB. Considering that fragment edges cover a total area of 176,555 Km^2 of Amazonian forests [35], edge effects on tree architecture and allometry could translate into a large component of fragmentation-related carbon losses.

The AGB decline near the edges creates an apparent contradiction with the higher Plant Area Index (PAI) found in these forest edges [24]. More specifically, Maeda and colleagues (2022) found PAI values - a combination of leaf and wood surface areas – to be higher near the forest edges due to a large increase in the density of small trees, despite a reduction of the upper canopy PAI caused by the mortality and damage of tall trees. This discrepancy can be explained by the disproportional contribution of tall trees to the aboveground forest biomass [54,55].Furthermore, the edges of these fragments are dominated by pioneer species with acquisitive traits [56], that thrive under the light-rich environment caused by lateral light penetration and by the formation of gaps associated with the mortality of large trees [57]. Traits of pioneer species include a larger volume per mass unit (low wood density) and large foliar area [58] which together increase the PAI of edge forests [59] without a concomitant increase in AGB.

The mechanisms that allow species to change their architecture remain elusive, as a shift in species composition may partly reflect architectural changes [56] We propose that future research on tree architecture should continue to untangle the interactions of the environment with functional diversity within species. TLS-based data combined with molecular, genetic and physiological processes regulating tree architecture can help resolve debates concerning the mechanisms by which trees change their architecture [1,60] and improve predictions of plant responses to global changes. TLS-based architectural data at the tree and species levels can help elucidate mechanisms controlling tree architecture in the Amazon such as (i) the specific environmental factors determining architectural variation, (ii) the molecular and physiological processes regulating tree architecture, and (iii) whether variation in architecture reflects genetic differences (high interspecific variation) or plastic responses to environmental heterogeneity (high within-species variation). This may help resolve the mechanisms by which species respond to global changes and improve predictions of the terrestrial carbon sink – or source - with increasing fragmentation.

METHODS

Study site and sampling design

The study was conducted in Central Amazonian forests (2°20 30 ′S, 60° 05 37 W) near Manaus, Brazil, in the reserves of the Biological Dynamics of Forest Fragments Project (BDFFP), the world's longest-running experimental study of habitat fragmentation[37]. The region has seen notable carbon and biodiversity losses due to forest fragmentation effects [35,56]. The BDFFP sites are composed of forest fragments originally isolated in 1980-1983 after the conversion of the surrounding mature forest into cattle pastures. Currently, the matrix surrounding the forest fragments is dominated by secondary growth forests, but a 100 m strip surrounding the forest fragments is cleared regularly by cutting vegetation regrowth to maintain their isolation (Supplementary Figure 1). As an experiment that minimises additional anthropogenic influences such as illegal logging, hunting, fire penetration and pollution, the project offers insights into ecological and environmental changes in fragmented forests. All trees that are in permanent plots within the BDFFP project.

For this study, we investigate how the architecture of trees varies with distance from the forest edge in four forest fragments across two regions in Central Amazonia (Dimona and Colosso; two of 1 ha, one of 10 ha and one of 100 ha reserves). The maximum distance from forest edges towards the forest interior varies between fragments, with 50 m for 1 ha fragments, 100 m for the 10-ha fragment and 500 m for 100 ha the fragment. Compared to undisturbed forests in the fragment interior, the forest near the edges is dominated by a higher density of early successional, fast-growing species because of elevated tree mortality and seed dispersal from degraded neighbouring habitats [37,56]. The edges of these fragments can have up to 5°C higher temperatures than the forest interior during the dry season [28]. During periods of lower precipitation in the region, the edges of these fragments have lower soil moisture, which creates periods of higher evaporative demand for tall trees

in the edges [28]. The fragment edges have a sparser upper canopy marked by lower plant area index (PAI) above 15 m in vertical height, which creates a light-rich environment and higher light availability in the understory of forest edges [24].

Terrestrial laser scanning: data acquisition and pre-processing

The three-dimensional structure of trees was assessed based on point-cloud data acquired using a state-of-the-art terrestrial laser scanning (TLS) system. The TLS data were acquired using a RIEGL VZ-400i system in April 2019 within the BDFFP permanent forest plots. We used a scan resolution of 40 mdeg in both azimuth and zenith directions, which results in a point spacing of 34 mm at 50 m distance from the scanner. The laser pulse repetition rate used was 600 kHz, allowing a measurement range of up to 350 m and up to eight returns per pulse. The scans covered three transects of 100 × 10 m and three transects of 50 × 10 m near the fragment edges and perpendicular to the forest fragment margins (Supplementary Figure 1). We also included one transect of 30 × 10 m length in the centre of the 100-ha forest fragment, which lies 500 m from any fragment margin to ensure sampling of forest interior in the absence of edge effects on tree architecture.

To ensure a full 3D representation of the upper canopy (maximum canopy height = 36 m), each transect consisted of three scan lines parallel to each other with scans spaced at 5 m intervals within and between lines. The distance between scanning positions was smaller than the 10–40 m usually applied in previous studies to minimise data uncertainties due to occlusion in dense tropical forests and maximise data acquisition in the upper canopy [61]. Given that the RIEGL VZ-400i has a zenith angle range of 30–130°, an additional scan was acquired at each sampling location with the scanner tilted at 90° from the vertical position. A total of 1,188 scans across all transects resulted in a complete sampling of the full hemisphere in each scan location. All scans were later co-registered into a single point cloud per transect using the RiSCAN PRO software version 2.9. Given that the RIEGL VZ-400i uses onboard sensor data with an algorithm to align scans without the use of reflectors, automatic registration was done before a final adjustment of scans. More details on how the data was used to investigate edge effects on structure and dynamics and the quality of the canopy point clouds can be found in Maeda and colleagues[24] and Nunes and colleagues [28], respectively.

Individual tree segmentation and quantitative structural modelling

Individual tree segmentation used an automatic approach followed by manual corrections. The automatic segmentation of individual trees was based on the shortest paths method by Raumonen and colleagues [62]. In this method, the shortest paths from the points to the base layer above the ground level are determined with restrictions on horizontal directions allowing better dealing with occluded regions and holding back paths going sideways into neighbouring trees. After the shortest paths were determined, the trees are defined as all points connected via shortest paths to the same stem section close to ground. The stem sections are iteratively

defined around the base layer points that are ranked by the number of shortest paths connected to the point. It started from the point with most paths, the stem section around was first defined, and proceeded with the next highest ranked point not yet assigned to a tree. Considering a reverse J-shaped distribution of tree size of Amazonian forests - with a decreasing density of individuals with increasing diameter at breast height (DBH) [63], we started the extraction of trees from the largest to smaller individuals within each transect to ensure that most large trees within the study area were included. However, some limits were imposed to the automatic approach, including 1) the dense canopy with trees occupying different strata, 2) the high diversity and variability in tree architecture, 3) the high abundance of lianas and 4) the noise in the data produced by wind flapping. Manual corrections to remove lianas and to identify extraneous and missing branches of trees represented a substantial fraction of the processing time. Trees that were severely damaged or dead, as well as trees whose crowns could not be clearly discerned from those of lianas or neighbouring trees were excluded from our analysis.

A total of 315 individual trees were segmented and extracted from the original TLS point clouds. A quantitative structure model (QSM) of the woody structure, proposed by Raumonen and colleagues [64], quantitatively describes the topological, geometric and volumetric properties of trees (Supplementary Figure 2). A QSM consists of a hierarchical collection of building blocks - usually geometric primitives such as cylinders and cones – which are fitted to the point clouds to locally approximate the woody parts. The use of circular cylinders in our study is a robust and accurate approach to estimate diameters, lengths, directions, angles and volumes [65]. Fitting cylinders to smaller branches, however, can lead to significant overestimation of the diameters and volumes stemming from the uncertainties of LiDAR measurements [66]. To reduce these uncertainties related to branch size, we followed Jackson and colleagues [44] and trimmed off branches with diameters < 2 cm from the QSMs. This procedure was reported to not affect the estimate of architectural traits across tropical forests [44]. QSMs provided estimates of branch size distribution, parent-child relations of the branches, diameters, lengths, angles, directions and volumes, which are key properties that can be used to estimate architectural traits [10]. Details of parameters for QSM reconstruction can be found in Supplementary Methods 1. The QSM database included trees that varied in DBH (2.4 - 72.3 cm), tree height (5.0 - 35.8 m) and volume (0.01 - 13.0 m^3) (Supplementary Figure 3).

Tree architectural traits

In this study, we propose that surface area per unit volume (m^2 m^{-3}) of branches and trunk, asymmetry [-], path fraction [-] and relative crown dimensions, including relative crown depth (m m^{-1}) and relative crown width (m cm^{-1}), are traits that may be sensitive to forest fragmentation, as they have been linked to maintenance costs for respiration, mechanical stability, hydraulic conductance and light capture. Retrieval of architectural traits are described in detail in Supplementary Methods 2. The ecological meaning of each architectural trait is synthesised in Table 1, and in more detail in Supplementary Methods 2.

Table 1. Traits, structural characteristics of trees with high trait values and their ecological meaning. This table summarises the information presented in more detail in the section "Tree architectural traits" of the Supplementary Methods 2.

Trait	**Structural characteristics**	**Ecological interpretation**
Branch or trunk surface area divided by branch or trunk woody volume	Trunk and branch thickness	High trait values indicate a higher proportion of metabolically inactive wood [6]. This is linked to lower support of aerial structures for light capture and productivity. On the other hand, higher values indicate higher interaction with the atmosphere, including higher respiration rates of the living tissues[5].
Relative crown width	Horizontal crown size in comparison to DBH	High trait values indicate trees that develop wide crowns, usually linked to limited access to light [67], although it can be limited by competition from neighbours [68]. Shade-tolerant trees can also expand their crowns to maintain minimal leaf overlap for light capture and withstand falling debris [69].
Relative crown depth	Vertical crown size in comparison to tree height, often caused by multi-stemming	In high-light environments trees invest in deep crowns to better compete with neighbours [17]. Multi-stemming also leads to large relative crown depths, as our algorithm also considers the crown as of the upper segments from any multi-stemming point.
Path fraction	Umbrella-shaped tree crown	Longer paths of trunks, branches and twigs prioritise sun exposure and light capture. This leads to longer water and nutrient transport distances that require high costs related to construction tissue [7]. High path fraction values represent umbrella-shaped crowns that prioritise sun exposure and light capture but are structurally expensive to build and are hydraulically less efficient [10].

Asymmetry	Wood allocation in branches and trunks shifted relative to the trunk's vertical axis	Asymmetrical crowns maximise capture of solar radiation by shifting their trunks and branches towards canopy gaps or away from their neighbours to avoid competition [45]. However, asymmetrical trees have lower mechanical stability and are more vulnerable to winds [30], which is a major cause of mortality of fragmented Amazonian forests [19].

Woody volume and allometric relationships

The accuracy of allometric models to predict aboveground biomass is crucial for terrestrial carbon stock mapping. Total tree height co-varies with bioclimatic stress that depends on temperature and precipitation variability [68,70], but little is known how forest fragmentation may affect these relationships. Locally derived DBH-height relationships improve existing allometric equations[70]. Differences in wood allocation in branches caused by fragmentation-related environmental changes may lead to differences in equations that predict woody volume as a function of DBH and total tree height [71]. In this paper, we investigated the effects of fragmentation on allometric relationships between DBH^2 H and woody volume, and also on allometric relationships between DBH and total woody volume, and discussed the implications of potential effects on the mapping of terrestrial carbon in fragmented forests. Woody volume, DBH and tree height were derived from the tree's QSMs. The QSM method can provide accurate woody volume estimates with no systematic bias regardless of the tree structural characteristics across tropical forests in Cameroon, Peru, Indonesia and Guyana [72,73]. Therefore, nondestructive estimates of woody volume from TLS can be a replacement for traditional sampling methods, and for updating allometry and reducing uncertainties in landscape-level biomass estimates[74]

Tree height to classify trees by time of establishment before or after forest fragmentation

Forest fragmentation may affect each architectural trait differently depending on the ontogenetic stage and tree size. As the fragment isolation occurred in 1980, the tall trees of our dataset are individuals that likely have survived the fragmentation effects, and differences in their architecture with forest fragmentation may reflect the ability of adult plants to acclimate to edge effects. On the other hand, short trees can be included in three groups: 1) < 30 years old recruits that have colonised the area after the establishment of the forest fragments; 2) surviving trees from understory species at varying ontogenetic stages; and 3) trees from slow-growing species, including upper canopy species at varying ontogenetic stages. Trees in group 1 have already been exposed to edge effects during their juvenile phase. Conversely, changes in the architecture of trees in groups 2 and 3 reflect acclimation of short-stature adult individuals to edge effects that, analogous to the tall surviving trees, change their architecture during the adult phase.

Long-term measurements from the BDFFP project since 1980 revealed that, among all the trees that have been tagged and monitored, all trees > 20 m in height have been growing in the BFFDP forest fragments before 1990 (Supplementary methods 3; Supplementary Figure 4), which indicates that trees > 20 m in height are those that have survived the fragmentation effects. Therefore, any change in the architecture of these tall trees must have occurred during their adult phase. Our data also indicated that ~ 33% of trees < 20 m in height have also been growing in these forests since before 1990. This suggests that 66% of the small trees < 20 m in height are new, young recruits (i.e., trees that have colonised these fragments within the last 30 years) that were exposed to edge effects already in their juvenile phase. We thus used 20 m tree height as a threshold separating early-successional short trees (< 20 m) and surviving adult trees (> 20 m).

Determining edge effects extent on architectural traits

Long-term studies from the BDFFP have demonstrated that edge effects vary widely in extent, with biophysical changes that can penetrate from 20 m to 300 m [37]. To estimate the extent of edge effects on each architectural trait, we used mixed linear models (LME, Eq. 1) that contained a variable representing the plot category of location near an edge or in the forest fragment interior (edge effects), following Nunes and colleagues [75]. The model also included a variable that represented tree height (H), considering that architectural traits co-vary with tree size and ontogenetic stage [10,76]. Edge effects and tree height were treated as additive terms to examine the significance of fragmentation and tree height on the variation of architectural traits. We also included an interaction term edge effects × tree height, as fragmentation may have different effects on trees of different heights (Eq. 5). To examine the influences of distance from edges on the allometric relationships between woody volume and DBH^2 H or woody volume and DBH, we tested how the log transformed variables interacted with edge effects (Eq. 6 and Eq. 7). Nested effects of forest site (Colosso versus Dimona sites), fragment size (1, 10 or 100 ha) and plot (or transect) identity were treated as random variables (μ), allowing us to account for the nested spatial variation in architectural traits and to include any idiosyncratic differences between forest site, fragment size and micro-environmental variation (i.e., topography, soil) between plots.

$$\text{Architectural trait} = \beta_0 + \beta_1 \times (\text{edge effects}) + \beta_2 \times \text{H} + \beta_3 \times (\text{edge effects}) \times \text{H} + \mu_i + \varepsilon_i \quad \textbf{(Eq. 5)}$$

$$\ln(\text{woody volume}) = \beta_0 + \beta_1 \times (\text{edge effects}) \times \ln(\text{DBH}^2\,\text{H}) + \mu_i + \varepsilon_i \quad \textbf{(Eq. 6)}$$

$$\ln(\text{woody volume}) = \beta_0 + \beta_1 \times (\text{edge effects}) \times \ln(\text{DBH}) + \mu_i + \varepsilon_i \quad \textbf{(Eq. 7)}$$

where β_0 to β_3 are the model parameters, μ_i is the random intercept for the nested effects of region i, fragment size i and plot identity i, and ε_i is the normally distributed residual error.

We then tested the influence of distance to edges on each architectural trait with distances to edges varying between 1 and 100 m, including tree woody volume. We then tested the influence of distance to edges, varying from 1 to 100 m, on each architectural trait; we determined the edge effects extent for each architectural trait based on the maximum absolute t-value of the term "edge effects" of the model (Supplementary Method 4; Supplementary Figure 5). The edge effects extent was then used to categorise our analysis into edge versus interior trees during all trait analyses.

We also examined the explained variance by the random variables of Eq.5 to investigate the spatial variability of architectural traits arising from region, landscape and plot (Supplementary Figure 6). The LME models were fitted using the lme function in the "nlme" R package.

Statistical modelling to predict edge effects on architectural traits

We used nonlinear mixed-effects models of architectural traits of trees in forest edges and trees in forest interior as a function of tree height (Equation 8). Allometric relationships between woody volume and $DBH^2 H$ or between woody volume and DBH were fitted using linear mixed models after log-transforming the dependent and independent variables [77] (Equations 9 and 10). We tested whether a quadratic term should be included to increase goodness-of-fitness of the allometric models by comparing each model's AIC (Supplementary Table 1). For all the models, plot identity nested within landscape (position of fragment within the landscape and fragment size) and region within Central Amazonia were included as random variables, allowing us to include any idiosyncratic differences between plots, fragments and regions. The models were fitted using the *nlme* function for the nonlinear mixed-effects model and *lme* function for the linear mixed-effects model in the "nlme" R package. Performance of the final models was also evaluated using an 80/20 split of the data for calibration and validation, respectively, over 200 randomised permutations of the dataset. These analyses generated a distribution of model coefficients and allowed an assessment of model stability and uncertainty of predictions.

$$\text{Architectural trait} = \beta_0 \,\text{Tree Height}^{\beta 1} + \mu_i + \varepsilon_i \qquad \textbf{(Eq. 8)}$$

$$\ln(\text{Woody volume}) = \beta_0 + \beta_1 \ln(DBH^2 H) + \beta_2 \ln(DBH^2 H)^2 + \mu_i + \varepsilon_i \qquad \textbf{(Eq. 9)}$$

$$\ln(\text{Woody volume}) = \beta_0 + \beta \ln(DBH) + \beta_2 \ln(DBH)^2 + \mu_i + \varepsilon_i \qquad \textbf{(Eq. 10)}$$

where β_0 to β_2 are the model parameters, μ_i is the random intercept for the nested effects of region i, fragment size i and plot identity i, and ε_i is the normally distributed residual error.

AGB calculation

Permanent plots within the BDFFP were distributed across a large area of 1,000 km2 in Central Amazonia. We used 36 permanent plots of 1 ha each in edge (30 ha) and interior forests (6 ha) to compile aboveground biomass (AGB) using data from Dimona, Colosso and Florestal. We then examined how edge effects on tree allometry control AGB relative to edge effects on forest structure (for example, edge effects on tree density and distribution of tree size caused by variations in tree mortality, growth and recruitment). We used diameter at breast height (DBH), defined as 1.3 m from the base of the stem, from 10,221 tree stems. For buttressed stems or other deformities, the point of measurement is raised above the deformity. All trees were distributed in 64 families, 242 genera and 953 species. Every plant was identified at the species level, or at least at the genus level. We then converted diameter measurements to woody volume estimates using the allometric equations 3 (interior forests) and 4 (edge forests), which predict woody volume as a function of DBH only. These models capture variation in woody volume related to tree height (i.e. tree damage and breakage) and fine-scale architectural variation (i.e. branch production, branch loss, branch and trunk thickening etc). To convert woody volume values to tree-level AGB, we used wood density values extracted from a global wood density database (https://datadryad.org/stash/dataset/doi:10.5061/dryad.234) [78], using the BIOMASS package in R. In cases where a stem was unidentified or where no taxon-specific wood density data were available, we applied the appropriate genus or family-specific wood density values. Aboveground biomass for each 1-ha plot was estimated as the sum of the tree-level AGB. Comparisons of plot-level AGB values using allometric equations specifically developed for edge forests versus interior forests allowed us to quantify the AGB variation owing to both structural changes at the forest level and allometric changes at the tree level caused by edge effects. Median AGB values and 95% confidence intervals were calculated for interior forests, as well as to edge forests using the allometric equation for interior forests (to capture edge effects on forest structure only) and to edge effects using the allometric equation for edge forests (to capture the combined edge effects on forest structure and tree allometry).

ACKNOWLEDGEMENTS

This study was funded by the Academy of Finland (decision numbers 318252, 319905 and 345472). This publication is number XXX of the Technical Series of the Biological Dynamics of Forest Fragment Forest (BDFFP – INPA / STRI). We thank the Biological Dynamics of Forest Fragments Project for the great logistical support in the field and the research assistance. Jérôme Chave acknowledges “Investissement d’Avenir” grants (CEBA, ref. ANR-10-LABX-25-01; TULIP, ref. ANR-10-LABX-0041). Jin Wu was supported by National Natural Science Foundation of China (#31922090), the Innovation and Technology Fund (funding support to State Key Laboratories in Hong Kong of Agrobiotechnology) of the HKSAR, China, and the Hung Hing Ying Physical Sciences Research Fund. Josep Peñuelas was supported by the TED2021-132627B-I00 grant, funded by MCIN and the European Union NextGeneration EU/PRTR, and the

CIVP20A6621 grant funded by the Fundación Ramón Areces. Gabriela Zuquim acknowledges the Academy of Finland (grant number 344733) and Danish Council for Independent Research – Natural Sciences (grant number 9040-00136B).

AUTHOR CONTRIBUTIONS

M.H.N. and E.E.M. conceived the study. M.H.N. and E.E.M. led TLS data collection in the field. J.L.C.C., W.F.L., A.A., B.V. and S.L. collected tree measurements data and identified tree specimens. M.H.N., P.R., T.J. and E.E.M. processed the LiDAR data. M.H.N. performed data analyses and wrote the manuscript. M.H.N., M.C.V, J.L.C.C., W.F.L., P.R., T.J., G.Z., J.W., J.P., J.C. and E.E.M. contributed to the revision of the paper.

COMPETING INTERESTS

The authors declare no competing interests.

REFERENCES

1. West, G. B., Enquist, B. J. & Brown, J. H. A general quantitative theory of forest structure and dynamics. *Proc. Natl. Acad. Sci. U. S. A.* **106**, 7040–7045 (2009).
2. Lines, E. R., Fischer, F. J., Owen, H. J. F. & Jucker, T. The shape of trees: Reimagining forest ecology in three dimensions with remote sensing. *J. Ecol.* **110**, 1730–1745 (2022).
3. Sheil, D., Salim, A., Chave, J., Vanclay, J. & Hawthorne, W. D. Illumination-Size Relationships of 109 Coexisting Tropical Forest Tree Species. *J. Ecol.* **94**, 494–507 (2006).
4. Robertson, A. L. *et al.* Stem respiration in tropical forests along an elevation gradient in the Amazon and Andes. *Glob. Chang. Biol.* **16**, 3193–3204 (2010).
5. Susan E. Trumbore, Alon Angert, Norbert Kunert, Jan Muhr & Jeffrey Q. Chambers. What's the flux? Unraveling how CO_2 fluxes from trees reflect underlying physiological processes. *New Phytol.* **197**, 353–355 (2013).
6. Reich, P. B. *et al.* Temperature drives global patterns in forest biomass distribution in leaves, stems, and roots. *Proc. Natl. Acad. Sci. U. S. A.* **111**, 13721–13726 (2014).
7. Smith, D. D. *et al.* Deviation from symmetrically self-similar branching in trees predicts altered hydraulics, mechanics, light interception and metabolic scaling. *New Phytol.* **201**, 217–229 (2014).
8. Owen, H. J. F., Flynn, W. R. M. & Lines, E. R. Competitive drivers of interspecific deviations of crown morphology from theoretical predictions measured with Terrestrial Laser Scanning. *J. Ecol.* **109**, 2612–2628 (2021).
9. Goodman, R. C., Phillips, O. L. & Baker, T. R. The importance of crown dimensions to improve tropical tree biomass estimates. *Ecol. Appl.* **24**, 680–698 (2014).

10. Malhi, Y. *et al.* New perspectives on the ecology of tree structure and tree communities through terrestrial laser scanning. *Interface Focus* **8**, 20170052 (2018).

11. Burt, A. *et al.* New insights into large tropical tree mass and structure from direct harvest and terrestrial lidar. *R Soc Open Sci* **8**, 201458 (2021).

12. Sussex, I. M. & Kerk, N. M. The evolution of plant architecture. *Curr. Opin. Plant Biol.* **4**, 33–37 (2001).

13. Negrón-Juárez, R. I. *et al.* Widespread Amazon forest tree mortality from a single cross-basin squall line event. *Geophys. Res. Lett.* **37**, (2010).

14. Hollender, C. A. & Dardick, C. Molecular basis of angiosperm tree architecture. *New Phytol.* **206**, 541–556 (2015).

15. Reis, C. R. *et al.* Forest disturbance and growth processes are reflected in the geographical distribution of large canopy gaps across the Brazilian Amazon. *J. Ecol.* **110**, 2971–2983 (2022).

16. Chambers, J. Q. *et al.* Respiration from a tropical forest ecosystem: Partitioning of sources and low carbon use efficiency. *Ecol. Appl.* **14**, 72–88 (2004).

17. Laurans, M. & Vincent, G. Are inter- and intraspecific variations of sapling crown traits consistent with a strategy promoting light capture in tropical moist forest? *Ann. Bot.* **118**, 983–996 (2016).

18. Ribeiro, G. H. P. M. *et al.* Mechanical vulnerability and resistance to snapping and uprooting for Central Amazon tree species. *For. Ecol. Manage.* **380**, 1–10 (2016).

19. Reis, S. M. *et al.* Climate and crown damage drive tree mortality in southern Amazonian edge forests. *J. Ecol.* **110**, 876–888 (2022).

20. Trumbore, S. Carbon respired by terrestrial ecosystems - recent progress and challenges. *Glob. Chang. Biol.* **12**, 141–153 (2006).

21. Valladares, F. & Niinemets, Ü. The architecture of plant crowns: From design rules to light capture and performance. in *Functional Plant Ecology* 101–150 (CRC Press, 2007). doi:10.1201/9781420007626-4.

22. Laurance, W. F. *et al.* Biomass Collapse in Amazonian Forest Fragments. *Science* **278**, 1117–1118 (1997).

23. Laurance, W. F., Delamônica, P., Laurance, S. G., Vasconcelos, H. L. & Lovejoy, T. E. Rainforest fragmentation kills big trees. *Nature* **404**, 836 (2000).

24. Maeda, E. E. *et al.* Shifts in structural diversity of Amazonian forest edges detected using terrestrial laser scanning. *Remote Sens. Environ.* **271**, 112895 (2022).

25. Poorter, L., Bongers, F., Sterck, F. J. & Wöll, H. Architecture of 53 Rain Forest tree species differing in adult stature and shade tolerance. *Ecology* **84**, 602–608 (2003).

26. Poorter, L., Bongers, L. & Bongers, F. Architecture of 54 moist-forest tree species: traits, trade-offs, and functional groups. *Ecology* **87**, 1289–1301 (2006).

27. Camargo, J. L. C. & Kapos, V. Complex edge effects on soil moisture and microclimate in central Amazonian forest. *J. Trop. Ecol.* **11**, 205–221 (1995).

28. Nunes, M. H. *et al.* Forest fragmentation impacts the seasonality of Amazonian evergreen canopies. *Nat. Commun.* **13**, 917 (2022).

29. Laurance, W. F. & Curran, T. J. Impacts of wind disturbance on fragmented tropical forests: A review and synthesis. *Austral Ecol.* **33**, 399–408 (2008).

30. Jackson, T. *et al.* A new architectural perspective on wind damage in a natural forest. *Front. For. Glob. Chang.* **1**, (2019).

31. Zuleta, D. *et al.* Damage to living trees contributes to almost half of the biomass losses in tropical forests. *Glob. Chang. Biol.* (2023) doi:10.1111/gcb.16687.

32. Poorter, L. Are species adapted to their regeneration niche, adult niche, or both? *Am. Nat.* **169**, 433–442 (2007).

33. Coelho de Souza, F. *et al.* Evolutionary heritage influences Amazon tree ecology. *Proc. Biol. Sci.* **283**, (2016).

34. Calders, K. *et al.* Laser scanning reveals potential underestimation of biomass carbon in temperate forest. *Ecol Sol and Evidence* **3**, (2022).

35. Silva Junior, C. H. L. *et al.* Persistent collapse of biomass in Amazonian forest edges following deforestation leads to unaccounted carbon losses. *Sci Adv* **6**, (2020).

36. Hansen, M. C. *et al.* The fate of tropical forest fragments. *Sci Adv* **6**, eaax8574 (2020).

37. Laurance, W. F. *et al.* An Amazonian rainforest and its fragments as a laboratory of global change. *Biol. Rev. Camb. Philos. Soc.* **93**, 223–247 (2018).

38. Disney, M. Terrestrial LiDAR: a three-dimensional revolution in how we look at trees. *New Phytol.* **222**, 1736–1741 (2019).

39. Stovall, A. E. L., Vorster, A., Anderson, R. & Evangelista, P. Developing nondestructive species-specific tree allometry with terrestrial laser scanning. *Methods Ecol. Evol.* (2022) doi:10.1111/2041-210x.14027.

40. Paciorek, C. J., Condit, R., Hubbell, S. P. & Foster, R. B. The demographics of resprouting in tree and shrub species of a moist tropical forest. *J. Ecol.* **88**, 765–777 (2000).

41. McDowell, N. *et al.* Mechanisms of plant survival and mortality during drought: why do some plants survive while others succumb to drought? *New Phytol.* **178**, 719–739 (2008).

42. Olson, M. E. *et al.* Plant height and hydraulic vulnerability to drought and cold. *Proc. Natl. Acad. Sci. U. S. A.* **115**, 7551–7556 (2018).

43. Vovides, A. G. *et al.* Change in drivers of mangrove crown displacement along a salinity stress gradient. *Funct. Ecol.* **32**, 2753–2765 (2018).

44. Jackson, T. *et al.* An architectural understanding of natural sway frequencies in trees. *J. R. Soc. Interface* **16**, 20190116 (2019).

45. Olivier, M.-D., Robert, S. & Fournier, R. A. Response of sugar maple (Acer saccharum, Marsh.) tree crown structure to competition in pure versus mixed stands. *For. Ecol. Manage.* **374**, 20–32 (2016).

46. Kunz, M. *et al.* Neighbour species richness and local structural variability modulate aboveground allocation patterns and crown morphology of individual trees. *Ecol. Lett.* **22**, 2130–2140 (2019).

47. Albiero-Júnior, A., Venegas-González, A., Camargo, J. L. C., Roig, F. A. & Tomazello-Filho, M. Amazon forest fragmentation and edge effects temporarily favored understory and midstory tree growth. *Trees* (2021) doi:10.1007/s00468-021-02172-1.

48. Koch, G. W., Sillett, S. C., Jennings, G. M. & Davis, S. D. The limits to tree height. *Nature* **428**, 851–854 (2004).

49. Leitold, V. *et al.* El Niño drought increased canopy turnover in Amazon forests. *New Phytol.* **219**, 959–971 (2018).

50. Laurance, W. F., Ferreira, L. V., Rankin-de Merona, J. M. & Laurance, S. G. Rain Forest fragmentation and the dynamics of amazonian tree communities. *Ecology* **79**, 2032–2040 (1998).

51. Laurance, W. F., Laurance, S. G. & Delamonica, P. Tropical forest fragmentation and greenhouse gas emissions. *For. Ecol. Manage.* **110**, 173–180 (1998).

52. Nascimento, H. E. M. & Laurance, W. F. Biomass dynamics in amazonian forest fragments. *Ecol. Appl.* **14**, 127–138 (2004).

53. Qin, Y. *et al.* Carbon loss from forest degradation exceeds that from deforestation in the Brazilian Amazon. *Nat. Clim. Chang.* **11**, 442–448 (2021).

54. Gora, E. M. & Esquivel-Muelbert, A. Implications of size-dependent tree mortality for tropical forest carbon dynamics. *Nat Plants* **7**, 384–391 (2021).

55. Fauset, S. *et al.* Hyperdominance in Amazonian forest carbon cycling. *Nat. Commun.* **6**, 6857 (2015).

56. Laurance, W. F. *et al.* Rain forest fragmentation and the proliferation of successional trees. *Ecology* **87**, 469–482 (2006).

57. Lohbeck, M. *et al.* Successional changes in functional composition contrast for dry and wet tropical forest. *Ecology* **94**, 1211–1216 (2013).

58. Malhado, A. C. M. *et al.* Spatial trends in leaf size of Amazonian rainforest trees. *Biogeosciences* **6**, 1563–1576 (2009).

59. Ma, L. *et al.* Characterizing the three-dimensional spatiotemporal variation of forest photosynthetically active radiation using terrestrial laser scanning data. *Agric. For. Meteorol.* **301-302**, 108346 (2021).

60. Savage, V. M. *et al.* Hydraulic trade-offs and space filling enable better predictions of vascular structure and function in plants. *Proc. Natl. Acad. Sci. U. S. A.* **107**, 22722–22727 (2010).

61. Wilkes, P. *et al.* Data acquisition considerations for Terrestrial Laser Scanning of forest plots. *Remote Sens. Environ.* **196**, 140–153 (2017).

62. Raumonen, P., Brede, B., Lau, A. & Bartholomeus, H. A Shortest Path Based Tree Isolation Method for UAV LiDAR Data. in *2021 IEEE International Geoscience and Remote Sensing Symposium IGARSS* 724–727 (2021). doi:10.1109/IGARSS47720.2021.9554346.

63. Vieira, S. *et al.* Forest structure and carbon dynamics in Amazonian tropical rain forests. *Oecologia* **140**, 468–479 (2004).

64. Raumonen, P. *et al.* Fast Automatic Precision Tree Models from Terrestrial Laser Scanner Data. *Remote Sensing* **5**, 491–520 (2013).

65. Åkerblom, M., Raumonen, P., Kaasalainen, M. & Casella, E. Analysis of Geometric Primitives in Quantitative Structure Models of Tree Stems. *Remote Sensing* **7**, 4581–4603 (2015).

66. Demol, M. *et al.* Volumetric overestimation of small branches in 3D reconstructions of Fraxinus excelsior. *Silva Fenn.* **56**, (2022).

67. Iida, Y. *et al.* Linking size-dependent growth and mortality with architectural traits across 145 co-occurring tropical tree species. *Ecology* **95**, 353–363 (2014).

68. Lines, E. R., Zavala, M. A., Purves, D. W. & Coomes, D. A. Predictable changes in aboveground allometry of trees along gradients of temperature, aridity and competition. *Glob. Ecol. Biogeogr.* **21**, 1017–1028 (2012).

69. Valladares, F., Skillman, J. B. & Pearcy, R. W. Convergence in light capture efficiencies among tropical forest understory plants with contrasting crown architectures: a case of morphological compensation. *Am. J. Bot.* **89**, 1275–1284 (2002).

70. Chave, J. *et al.* Improved allometric models to estimate the aboveground biomass of tropical trees. *Glob. Chang. Biol.* **20**, 3177–3190 (2014).

71. Martin-Ducup, O. *et al.* Terrestrial laser scanning reveals convergence of tree architecture with increasingly dominant crown canopy position. *Funct. Ecol.* **34**, 2442–2452 (2020).

72. Takoudjou, S. M. *et al.* Using terrestrial laser scanning data to estimate large tropical trees biomass and calibrate allometric models: A comparison with traditional destructive approach. *Methods in Ecology and Evolution* **9**, 799–1156 (2018).

73. Gonzalez de Tanago, J. *et al.* Estimation of above-ground biomass of large tropical trees with terrestrial LiDAR. *Methods Ecol. Evol.* **9**, 223–234 (2018).

74. Stovall, A. E. L., Anderson-Teixeira, K. J. & Shugart, H. H. Assessing terrestrial laser scanning for developing non-destructive biomass allometry. *For. Ecol. Manage.* **427**, 217–229 (2018).

75. Nunes, M. H. *et al.* Recovery of logged forest fragments in a human-modified tropical landscape during the 2015-16 El Niño. *Nat. Commun.* **12**, 1526 (2021).

76. Verbeeck, H. *et al.* Time for a plant structural economics spectrum. *Front. For. Glob. Chang.* **2**, (2019).

77. Chave, J. *et al.* Tree allometry and improved estimation of carbon stocks and balance in tropical forests. *Oecologia* **145**, 87–99 (2005).

78. Zanne, A. E. *et al.* Towards a worldwide wood economics spectrum. (2009) doi:10.5061/dryad.234.

Supplementary Files

This is a list of supplementary files associated with this preprint. Click to download.

- SupplementaryInformation.pdf